

## On the effect of phase transition on impact pressures due to sloshing

J.-P. Braeunig<sup>(1)</sup>, L. Brosset<sup>(2)</sup>, F. Dias<sup>(3,4)</sup>, J.-M. Ghidaglia<sup>(3)</sup>

<sup>(1)</sup>INRIA Nancy-Grand Est, Equipe CALVI

Villers-lès-Nancy, France

<sup>(1)</sup>CEA DIF

Arpajon, France

<sup>(2)</sup>Liquid Motion Dept, GTT (Gaztransport & Technigaz)

Saint-Rémy-lès-Chevreuse, France

<sup>(3)</sup>CMLA Centre de Mathématiques et de Leurs Applications, Ecole Normale Supérieure de Cachan and CNRS

Cachan, France

<sup>(4)</sup>School of Mathematical Sciences, University College Dublin, Dublin, Ireland

### ABSTRACT

Sloshing assessment for a new membrane LNG vessel relies on Sloshing Model Tests (SMT) at small scale (scale 1:40 most of the time) with 6 degree-of-freedom excitations reproducing the full-scale-ship motions by Froude-scaling. Numerous local physical phenomena involved during each impact do not follow a Froude similarity.

GTT, in a patient R&D effort, aims to study each of them one after the other, in order to limit the biases induced by the experimental modeling.

Recent studies on the Density Ratio (DR) between the gas and the liquid (Maillard *et al.*, 2009) and on the compressibility of the gas phase (Braeunig, Brosset, Dias, Ghidaglia, 2009) have led GTT to use systematically a heavy mixture of gases instead of air during its SMT in order to match the DR with the real one on board LNG carriers and reduce the compressibility bias.

In this communication, the objective is to address, in the context of sloshing impacts, the complex situation of phase transitions between a liquid and its vapor in thermo-dynamical equilibrium along the phase boundary, as it is the case within tanks of LNG carriers.

Through a simple 1D semi-analytical model of a gas pocket compression, the influence of phase transition is analysed in the context of general fluids with application to LNG/NG, different thermal boundary conditions and different scales.

The model is first requested to explain qualitatively the trends observed experimentally during SMT with water and steam in a pressure vessel: the significant reduction of the statistical impact pressures and the disappearance of the pressure oscillations when gas-pocket impacts occurred.

**KEY WORDS:** Sloshing, LNG, phase transition, condensation, model test, scaling law, dimensionless number, compressibility.

### NOMENCLATURE

*ms, fs*: model scale, full scale

$\lambda$ : ratio between the full scale size and the model size  
 $k=L$  or  $k=G$  refers respectively to Liquid or Gas.

$\rho_k, p_k, T_k, C_k$ : density, pressure, temperature, speed of sound

$\tau_k, e_k, h_k, s_k, g_k$ : specific vol., energy, enthalpy, entropy, Gibbs potential

$P_{sat}, L$ : saturation pressure, latent heat

$\gamma$ : adiabatic constant for the gas

$g$ : acceleration due to gravity (9.81 m/s<sup>2</sup>)

Fr: Froude number

DR: Density Ratio between gas and liquid in a tank

Ja: Jakob number

CFS, PFS: Complete Froude Scaling, Partial Froude Scaling

SoS, EoS, SMT: Speed of Sound, Eq. of State, Sloshing Model Tests

LNG, NG: Liquefied Natural Gas, Natural Gas

### INTRODUCTION

Several physical phenomena occur locally, almost simultaneously, when a sloshing impact happens in a tank of a LNG carrier. The impact pressures that they induce can be very sharp in space and time and extremely sensitive to the variations of their initial conditions, the local inflow conditions. This explains the highly stochastic behavior of the maximum impact pressures recorded during Sloshing Model Tests (SMT). This also shows a necessary requirement for a good modeling of full scale sloshing by SMT: the sample of local inflow conditions for the impacts should be similar at both scales in order for the statistical pressures derived from this sample to be representative. As the global flow, which defines the impact inflow conditions, is ruled firstly by the Froude number and secondarily by the Density Ratio (DR) between the ullage gas and the liquid in the tank, it is generally assumed that the requirement is fulfilled when the model tank excitations are Froude-scaled from the full scale ones and when the DR is kept at the same level in the model tank as in the LNG tank.

These physical phenomena can be sorted in three different categories:

- *Incompressible dynamics* that includes the interaction between the liquid and the rigid structure (excluding the shock waves) and the interaction between the liquid and the gas while the gas remains incompressible. These phenomena are ruled by Froude number and

the DR.

- *Compressible dynamics* that includes the global compression of the escaping gas or the entrapped gas fractions (pockets or bubbles) and the local compression in both the liquid or the gas due to shock waves. These phenomena are ruled by Mach numbers.
- *The others* that include the phase transition for fluids coexisting along the phase boundary and hydro-elasticity interactions. Both of them are disregarded during SMT.

These phenomena have different relative influences for different impacts and even for a given impact at different locations. This is a major obstacle for any possibility of pressure scaling.

One of the main R&D area of GTT is to address the scaling issue by studying the different families of local phenomena one after the other, in order to better understand the physics behind and to improve as far as possible the experimental modeling.

Many efforts have been made on the compressibility effects recently (see Faltinsen & Timokha, 2009). We have presented last year (Braeunig, Brosset, Dias, Ghidaglia, 2009) our main conclusions on this subject. The concepts of *Partial Froude Scaling* (PFS, Froude scaled excitations but improperly scaled properties for the fluids) and *Complete Froude Scaling* (CFS, Froude-scaled excitations and properly scaled properties for the fluids) have been introduced. It has been shown theoretically and numerically that only a CFS can lead to a relevant Froude-scaling of the impact pressures. Unfortunately, there are no real fluids enabling an appropriate scaling of the fluid properties of LNG and NG at small scale. So a PFS, inducing a so-called *compressibility bias*, cannot be avoided during SMT. GTT's objective is to reduce as much as possible this bias.

The focus is now the phase transition influence on sloshing loads. This paper presents some preliminary findings.

SMT in a pressure vessel, with water and steam along the phase boundary, had been conducted in 2007. Results have been presented by Maillard *et al.* (2009). They showed that the phase transition has a significant influence on the statistical pressures. Furthermore this influence changes radically the pressure signature of pressure transducers located within vapor pockets, damping drastically the inevitable oscillations that would occur in the same situation with a non-condensable gas.

These results raised the following questions:

- How can the phase transition kill the pressure oscillations within gas pockets and reduce statistically the impact pressures?
- Is the phase transition an amplifying or a mitigating effect for the sloshing loads with LNG/NG at full scale?
- Are the notions of PFS and CFS extendable to the phase transition phenomenon?

A 1D semi-analytical model of a gas pocket compression has been developed including thermo-dynamical properties enabling the phase transition in order to give some insight into this problem and bring preliminary answers.

## PHYSICS OF SLOSHING IMPACTS

### Liquid impact phenomenology

During a sloshing impact within a tank of a LNG carrier several phenomena may happen locally simultaneously or sequentially. Six main phenomena have been described in Braeunig, Brosset, Dias, Ghidaglia, (2009) and referred to as **P<sub>1</sub>** to **P<sub>6</sub>**. **P<sub>1</sub>**, **P<sub>2</sub>**, **P<sub>4</sub>** and **P<sub>5</sub>** are related to:

- the change of momentum of the liquid due to the transfer to the gas and the change of shape of the liquid in order to avoid the obstacle.

- the compressibility effects mainly into the gas fraction but also into the liquid (shock wave).

These last effects were the main focus of Braeunig's paper. The **P<sub>3</sub>** phenomenon is the phase transition. It includes both the possible condensation of the gas fraction while compressed and the evaporation of the liquid while heated. Depending on the thermodynamics of the impact, one or both of these phenomena may happen when the gas fraction entrapped during an impact is compressed.

Studying the influence of this effect at different scales is our main objective here. The hydro-elasticity influence during the fluid-structure interaction (referred to as **P<sub>6</sub>**) is disregarded in this study in the same way as it is disregarded during classical SMT.

### Dimensionless numbers and scaling laws

Studying sloshing by model tests at small scale corresponds to using an experimental modelling of the reality. How close to the reality is this modelling?

For each impact the weight of the different local phenomena described in the previous sub-section is different. The best mathematical tool for tuning or checking the balance between two physical phenomena is the associated dimensionless number that should be kept constant at both scales. Obviously, keeping the right balance between a series of couples of physical phenomena will impose the right balance between all the phenomena together.

For a good experimental modelling the similarity of the global flow at both scales is a necessary starting point. Assuming that the global flow, neglecting at first the interactions between the liquid and the gas, is governed by the gravity and the inertial accelerations, the balance between hydrodynamic pressures  $\rho_L U^2$  and hydrostatic pressures  $\rho_L g L$  must be kept constant at both scales. This corresponds to the Froude scaling law:  $\rho_L U^2 / \rho_L g L = U^2 / g L = Fr^2$ ,  $U$  being a reference velocity.

Assuming the geometrical model scale is  $1/\lambda$ , the Froude scaling can be obtained only if the time model scale is  $1/\sqrt{\lambda}$ . So, during model tests the imposed motions of the model tank are deduced from those calculated at scale one by complying with both these geometrical and time scalings.

Now, for a perfect experimental modelling the balance between the different physical phenomena (at least **P<sub>1</sub>** to **P<sub>6</sub>**) involved locally during the impacts should be the same at both scales. It has been theoretically demonstrated by Braeunig, Brosset, Dias, Ghidaglia and Maillard (2010) from the three conservation equations (mass, momentum and energy) that the only way to have this right balance for **P<sub>1</sub>**, **P<sub>2</sub>**, **P<sub>4</sub>**, **P<sub>5</sub>** at both scales, namely the escape of the gas and the compressibility effects of both the gas and the liquid, is to impose at both scales the same DR between the gas and the liquid and to have also the Equations of State (EoS) in Froude agreement in both the gas and the liquid. In that case, assuming that no other phenomena are involved, the impact pressures can be scaled by:  $p^{fs} = (\rho_L^{fs} / \rho_L^{ms}) \cdot \lambda \cdot p^{ms}$  (1)

A more intuitive way to understand this need to Froude-scale the EoSs is to come back to the dimensionless numbers. The dimension of the pressure into a compressed gas pocket is that of  $\rho_L U C_G$ . Assuming the right influence of the gas compressibility leads to keep the ratio between hydrodynamic pressure and gas pocket pressures constant at both scales, namely fulfil the Mach similarity for the gas:  $\rho_L U^2 / \rho_L U C_G = U / C_G = (Mach)_G$ . As  $U$  is already committed to Froude-scale, the only way to fulfil the  $(Mach)_G$  similarity is to Froude-scale also  $C_G$ . Doing so, the **P<sub>2</sub>** phenomenon (compression of the gas fraction) would be adequately taken into account at model scale.

Similarly, for a good balance of the shock phenomena **P<sub>5</sub>** at small scale, the Mach similarity for liquid, understood as the ratio between

hydrodynamic pressures and acoustic pressures  $\rho_L UC_L$  must be also fulfilled:  $\rho_L U^2 / \rho_L UC_L = U/C_L = (\text{Mach})_L$ . With the same reasoning as for the gas, the only way to fulfil the  $(\text{Mach})_L$  similarity is to Froude-scale also  $C_L$ .

Furthermore, the viscosity of the liquid is considered to be of small influence during impact but, if one wanted to take this influence correctly at small scale, fulfilling additionally the Reynolds scaling law would be required. This would lead to  $v_{ms} = \lambda^{3/2} \nu_{fs}$ ,  $\nu$  being the kinematical viscosity.

For each additional physical phenomenon one wants to include in the impact process, the only way to fulfil the corresponding new scaling law is to fix new gas and/or liquid properties at small scale. The liquid and gas allowing this *Complete Froude Scaling* of the impact pressures do not exist in the nature but the bias induced by a *Partial Froude Scaling* can be studied with numerical simulations with ideal properties for the fluids.

It will be shown in the next section that these CFS and PFS notions can be extended to the phase transition phenomenon by means of the Jakob dimensionless number.

## INFLUENCE OF THE PHASE TRANSITION ON SLOSHING

Maillard *et al.*, (2009) presented SMT in a pressure vessel enabling testing water and its vapor along the phase boundary. A large range of temperatures and pressures, hence DRs have been studied for the same harmonic excitation and the same filling level. Some tests have been repeated but with water and different non-condensable mixtures of gases at ambient conditions of temperature and pressure. A few conclusions have been deduced from the results concerning the influence of the phase transition on sloshing. The conclusions are summarized below. Our main objective in the present paper is to explain the physics behind these trends.

The statistical pressure vs. DR is given in Figure 1.

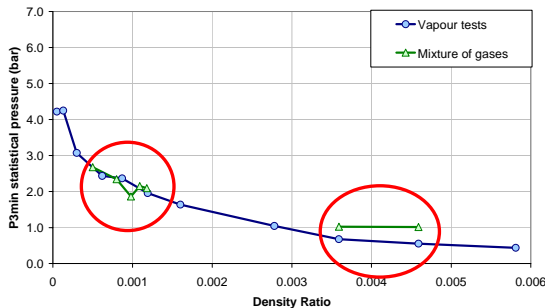


**Fig. 1** – Maximum expected pressure after 3 min. vs. Density Ratio

For the two testing principles (1/water and a mixture of gases (in green on Figure 1), 2/ water and its vapor along the phase boundary (in blue on Figure 1)) there is a strong decrease of the statistical pressure when the density ratio increases. Regardless of the testing principles, the results for density ratios from 0.0005 to 0.0012, present values in total agreement and it is quite difficult to distinguish between the two curves. Nevertheless, for the highest density ratios (>0.003), results present some discrepancies between the two testing conditions. The statistical pressures are slightly reduced when phase transition is possible.

A tentative explanation is given by the authors: *the fraction of gas is condensing during the sloshing events with water vapor mitigating the compressibility effects. Vapor pockets behave like punctured balls under the liquid impacts. The peak pressure could then be reduced.* Moreover this effect should be significant as it more than compensates the influence of the compressibility difference between the two gases at

the same DR, which would lead to the opposite trend without condensation.

This phenomenon is visible only for high DRs, around the actual DR value within the tanks of LNG carriers ( $4 \cdot 10^{-3}$ ) for which the compressibility effects are important. On the contrary, for low DRs, the gas can escape more easily and the compressibility effects are less important. The phase transition influence seems then to be insignificant.

One other interesting result was mentioned: for the two test principles the gas pocket events can be sorted easily from the pressure signatures: the pressure sensors within the pocket have almost exactly the same pressure signal. Nevertheless the pressure signatures are completely different with non-condensable gas than with vapor as shown in Figure 2.

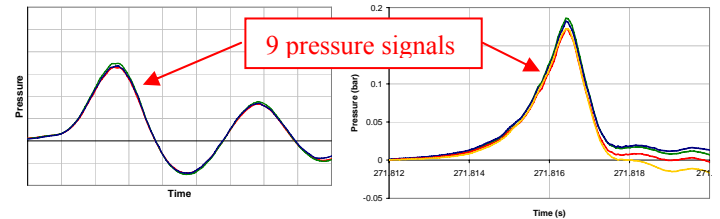


**Fig. 2** - Pressure signature for a gas pocket impact during sloshing tests

The gas pocket events with non-condensable gases present strong oscillations of the pressure signal, the frequencies of which are related to the compressibility modulus of the gas, hence to its SoS. On the contrary these oscillations are totally absent (or strongly damped) for tests with vapor although there are many such events.

These phenomena happen during a period corresponding to a sloshing pressure pulse. The order of magnitude of the duration is 1 ms at small scale. The dynamics of the condensation is thus very important.

It seems reasonable to consider that the phase transition is the cause of the effects that have been described in this sub-section. The influence is clearly associated to the compression of the gas phase. Whether what happens is condensation or not, is for the time being only a conjecture.

As the compressibility bias observed during model tests favours the compressibility effects, the phase transition effects could be mitigated when full scaled.

## THE PHASE TRANSITION PHENOMENON

### Preliminary notions about phase transition

Let us consider the case of a *pure substance* in a region where two phases at most coexist: liquid and gas. Then, there exist three regions in the  $(p, T)$  diagram (see Figure 3): the liquid region, the gas region and the fluid region. The critical point  $(p_c, T_c)$  separates the three regions. The vapor curve separates the liquid and gas regions for  $p < p_c$  and  $T < T_c$ . It is an increasing curve named saturation curve and denoted by  $p = P_{sat}(T)$ .

The values of critical temperatures  $T_c$  et pressures  $p_c$  for water and methane are respectively  $T_c \cong 647 \text{ K}$ ,  $p_c \cong 221 \text{ bar}$ ,  $T_c \cong 191 \text{ K}$ ,  $p_c \cong 46 \text{ bar}$ . For sloshing inside LNG tanks,  $p \ll p_c$  and  $T \ll T_c$ .

Therefore, only the liquid and gas regions separated by the saturation curves are to be considered. In both regions the fluids have proper EoSs:  $\rho_k = R_k(p, T)$ ,  $e_k = E_k(p, T)$ , ( $k=L$  or  $G$  for respectively liquid or gas) and all the thermo-dynamical properties are discontinuous across the saturation curve.

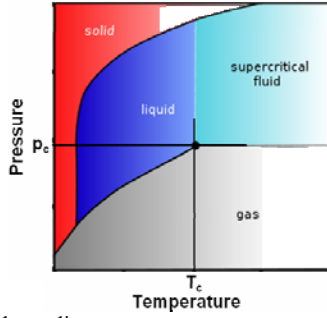


**Fig. 3** – Typical phase diagram

Along this curve one has Clapeyron's relation:

$$T \frac{dP_{sat}}{dT}(T) = \frac{L(T)}{\tau_{G,sat}(T) - \tau_{L,sat}(T)} \quad (2)$$

$\tau_{k,sat}(T)$  denotes the specific volume of the phase  $k$  on the saturation curve:

$$\tau_{k,sat}(T) = 1 / \rho_k(P_{sat}(T), T) \quad (3)$$

$L(T)$  is the latent heat:  $L(T) = h_G(P_{sat}(T), T) - h_L(P_{sat}(T), T)$  (4),

where  $h_k(p, T)$  is the specific enthalpy of phase  $k$ . The dimensionless

$$\text{number} \quad Ja(T) = \frac{h_G(P_{sat}(T), T)}{h_G(P_{sat}(T), T) - h_L(P_{sat}(T), T)} \quad (5),$$

known in the literature as the *Jakob* number, measures the ratio of the sensible heat to latent heat  $L$ .

For water, Jakob number at atmospheric pressure is  $Ja = 1.15$  while for Methane  $Ja = 1.56$ . As far as phase transition is concerned, two pure substances will behave likewise when their Jakob numbers are almost equal. So the behavior should be different for water and methane.

### Boundary condition at a free surface

Let us consider a free surface separating the two phases both considered as compressible fluids. In the bulk of each phase the complete Euler equations can be written as:

$$\frac{\partial \rho}{\partial t} + \text{div}(\rho \cdot u) = 0 \quad (6)$$

$$\frac{\partial(\rho \cdot u)}{\partial t} + \text{div}(\rho \cdot u \otimes u) + \text{grad}(p) = \rho \cdot g \quad (7)$$

$$\frac{\partial(\rho \cdot E)}{\partial t} + \text{div}(\rho \cdot H \cdot u) = \rho \cdot g \cdot u \quad (8)$$

$E$  is the total specific energy,  $H$  is the total specific enthalpy, and  $u$  is the three-dimensional velocity vector. The equation of the surface separating the two fluids is denoted by  $\eta(x, t) = 0$ , the rate of production of fluid  $k$  at the interface is denoted by  $J_k = \rho_k(u_k - u_{int}) \cdot n_k$  (9)

where  $u_{int}$  denotes the velocity of the interface and  $n_k$  the unit normal at the interface pointing out of phase  $k$ .

$$\text{Mass conservation implies that} \quad J_G + J_L = 0 \quad (10)$$

and the standard kinematic conditions reads:

$$\rho_k \left( \frac{\partial \eta}{\partial t} + u_k \cdot \nabla \eta \right) + J_k |\nabla \eta| = 0 \quad (11)$$

On the other hand, following Ishii and Hibiki (2006), we have on the interface the three thermo-dynamical relations:

$$T_G = T_L, \quad P_G = P_L - J_G^2 \left( \frac{1}{\rho_G} - \frac{1}{\rho_L} \right), \quad g_G = g_L - \frac{J_G^2}{2} \left( \frac{1}{\rho_G^2} - \frac{1}{\rho_L^2} \right) \quad (12),$$

$$\text{where } g_k \text{ is the Gibbs potential:} \quad g_k = e_k - T_k s_k + \frac{p_k}{\rho_k} \quad (13)$$

$e_k$  denoting the specific energy and  $s_k$  denoting the specific entropy.

### Invariance of the equations under a change of scales

In Braeunig *et al.*, (2010) two dimensionless parameters  $\lambda$  and  $\mu$  were introduced, respectively the inverse of the geometrical scale ( $\lambda = L^s/L^{ms}$ ) and the liquid density scale ( $\mu = \rho_L^{ms}/\rho_L^s$ ). As shown in that paper, the system of equations (6), (7), (8) is invariant by these changes of scales provided that both equations of state  $\rho_k = R_k(p, T)$ ,  $e_k = E_k(p, T)$ , for  $k=G$  (gas) or  $L$  (liquid), are scaled as follows:

$$p \rightarrow \lambda \cdot p / \mu, \quad e \rightarrow \lambda \cdot e, \quad \rho \rightarrow \mu \rho \text{ and } T \rightarrow T.$$

Extending the approach to the case with phase transition, one can then show that these changes of variables leave the four previous boundary conditions (11), (12) invariant and amount to preserve the Jakob number  $Ja$ . In the absence of phase transition, this invariance amounts to preserve the Froude number, the density ratio and the Mach number. When including phase transition, scale invariance of the equations leads to preserve the Jakob number in addition.

Preserving the whole set of dimensionless numbers leads to similar results at both scales, while preserving all the aforementioned dimensionless numbers but the Jakob number leads to different results (phase transition bias).

The present discussion does not address the case of boundary conditions but only the bulk of the flow. For example, in case of a wall, heat exchanges with the outside can impact significantly the phase transition inside. In such a case, the external temperature and the wall conductivity (see e.g. equation (20)) will lead to supplementary dimensionless numbers.

In the following sections an exemplification of this proposition is presented by using a semi-analytical model for solving an academic 1D problem of gas pocket compression.

### Thermodynamics of water and LNG

During the compression of the gas fraction entrapped by sloshing impacts, the temperature and the pressure  $p(T)$  of the gas increase. The boundary between liquid and gas also evolves with  $P_{sat}(T)$ . So, adopting the relevant EoSs and saturation laws is crucial in order to understand what happens really.

**LNG** is not a pure substance but a mixture with a predominant proportion of Methane (typically more than 90%) complemented by Ethane, Propane, Nitrogen, etc. For such a mixture the phase transition phenomenon is complex and during the transition the temperature can vary as the composition evolves. In this paper since we are primarily interested in qualitative results, we shall only deal with pure Methane.

**Water or Methane** is classically studied with one of the two following approaches for a relevant approximation of the EoS in each fluid. The first one relies on high degrees polynomials fitted on experimental data (e.g. Faghri and Zhang, 2006). The second consists in using linearized EoSs in a limited range. For liquid water one can use a stiffened-gas-like EoS:

$$p + \pi = (N-1) \rho_L (e_L + e^*), \quad N(e_L + e^*) = C_{V,L} T - \pi / \rho_L \quad (14),$$

while for the gas a perfect gas law can be used :

$$p = (\gamma - 1) \rho_G e_G, \quad e_G = C_{V,G} T$$

Concerning the saturation curve, Antoine's law seems to be convenient:

$$p_{sat}(T) = P_0 \exp \left( \beta \left( \frac{1}{T_0} - \frac{1}{T} \right) \right) \quad (16),$$

$$\text{with} \quad \beta = \frac{\gamma}{\gamma - 1} \frac{T_0}{Ja} \quad (17)$$

Table 1 and Table 2 summarize the relevant characteristics of respectively the liquids and the gases of interest in this study.

**Table 1** – Characteristics of liquids at  $P_0 = 1 \text{ atm}$ .

Liquid I.S. Units	$T_0$	$\rho_{0L}$	N	$\pi$	$e^*$	$C_{V,L}$	$\beta$
Methane	111.6	423	4.63	$1.22 \cdot 10^9$	66231	7130	174
Water	373.15	958	1.89	$2.29 \cdot 10^9$	$2.98 \cdot 10^7$	7170	4966

**Table 2** – Characteristics of gas at  $P_0 = 1 \text{ atm}$ .

Gas I.S. Units	$T_0$	$\gamma$	$C_{V,G}$	$\beta$
Methane	111.6	1.3	4193	174
Steam	373.15	1.3	6715	4966

## A SIMPLE 1D PROBLEM OF GAS POCKET COMPRESSION

Before undertaking difficult and expensive new experiments as for instance new steam SMT or even LNG/NG SMT, GTT would like to know better whether phase transitions are likely to matter at full scale with the real fluids. It is believed that academic simplified versions of complex physical problems are helpful to give some insight.

A 1D problem of gas compression will be tentatively studied by a semi-analytical model.

### Reference problem description

The 1D problem presented here is based on the geometry of the 1D reference case proposed for the numerical benchmark study of ISOPE 2010 (see Dias *et al.*, 2010). It corresponds to the free fall of a liquid segment along a vertical line (1D tank). At the initial instant the liquid is at rest and is surrounded by a gas above and underneath it, at atmospheric pressure, as represented in Figure 4 at scale 1.

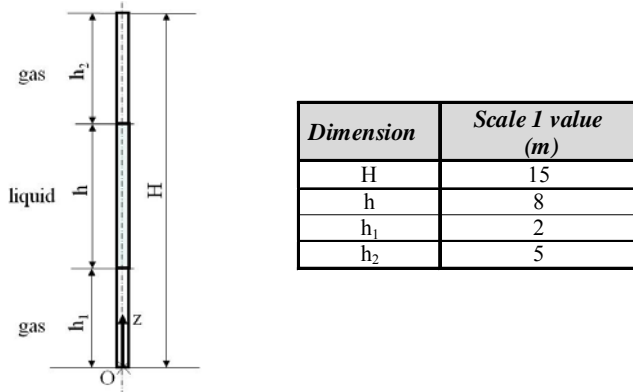


**Fig. 4** – Main characteristics of the reference problem

No flow outside of the line direction is allowed. This corresponds to an idealization of the free drop of a liquid piston within a vertical cylinder, very close to the Bagnold problem (Bagnold, 1939).

If the liquid were to be surrounded by vacuum instead of gas, the impact velocity would be 6.26 m/s at full scale (0.99 m/s at scale 1:40). The free fall would last 0.639 s.

This reference problem is studied under different variations, changing the liquid and gas in presence or the scale. Two scales are considered: full scale and a scale 1:40 corresponding to the scale adopted in GTT for SMT. For the liquid and gas properties two possibilities are considered: water and steam or LNG and vapor. In both cases the condition along the phase boundary with phase transitions and the condition without any possibility of phase transition are studied. Furthermore, different thermal boundary conditions are evaluated.

## Phenomenological analysis

From Figure 3 it appears that, if considering a particle of gas in conditions close to saturation, it will transform to liquid when the pressure is increasing at constant pressure or when the temperature is decreasing at constant pressure. For a particle of liquid, it evaporates into gas when the pressure decreases at constant temperature or when the temperature increases at constant pressure.

For the problem of a compressed gas pocket, both the pressure and the temperature inside the pocket increase according to the EoS. At the same time the boundary point between liquid and gas moves on the saturation curve  $P_{sat}(T)$ .

What matters here is clearly the comparison of slopes between  $p(T)$  and  $P_{sat}(T)$ . For a compressed gas particle:

$$\text{If } \frac{\partial p}{\partial T} < \frac{\partial P_{sat}}{\partial T} \rightarrow \text{no possible condensation}$$

$$\text{If } \frac{\partial p}{\partial T} > \frac{\partial P_{sat}}{\partial T} \rightarrow \text{condensation} \rightarrow \text{pressure comes back to } P_{sat}$$

The second situation is a good candidate for being the *oscillation killer* observed during the steam SMT. The semi-analytical model described below decomposes each time step in these two different phases. A purely mechanical phase enables locally the gas pressure to overcome slightly  $P_{sat}$ . The gas condensate during a thermo-dynamical phase and the pressure comes back to  $P_{sat}$ .

### Which thermo-dynamical boundary condition at the wall?

If we consider purely adiabatic conditions for a perfect gas during the compression of the gas fraction, it comes:

$$p(T) = p_0(T/T_0)^{\gamma/(\gamma-1)} \quad (18)$$

$p(T)$  can thus be directly compared with  $P_{sat}(T)$  given by Antoine's law (16). Results are shown in Figure 5 for methane and for water + steam in the vicinity of  $(p_0, T_0)$ , considering the conditions given in Tables 1 and 2.

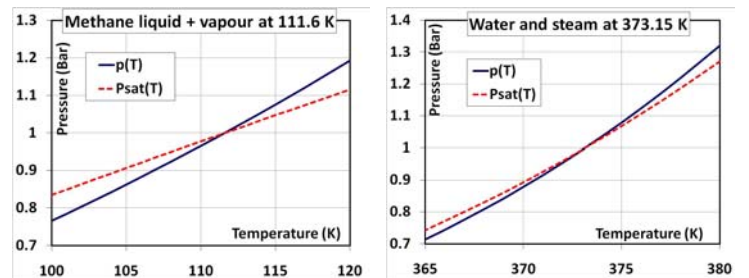


**Fig. 5** – Comparison of  $p(T)$  for a perfect gas in adiabatic conditions and  $P_{sat}(T)$  given by Antoine's law (16) for  $\text{CH}_4$  at 111.6 K (left) and water + steam at 373.15 K (right) –  $p_0 = 1 \text{ atm}$

For both pairs of fluids, condensation is possible since  $\frac{\partial p}{\partial T} > \frac{\partial P_{sat}}{\partial T}$

Nevertheless, the difference of slopes is larger for methane than for water and steam as the concavity of the curves  $p(T)$  and  $P_{sat}(T)$  are different for  $\text{CH}_4$ , while they are the same for water and steam. So, larger attenuations of the pressure oscillations are expected in vapor methane pockets than in steam pockets for Froude-similar inflow conditions.

We can now wonder whether a possible heat transfer at the wall is favourable or not for the condensation.

Goldstein (1964) performed experiments in a shock tube, compressing a steam pocket in thermo-dynamical equilibrium with water. He observed that a thin layer of water appeared at the wall during the compression and explained that this was possibly due to the heat transfer at the wall favouring a thermal boundary layer.

The phenomenon can intuitively be understood considering that in the thermal boundary layer,  $P_{sat}(T)$  will be smaller than in the pocket, whilst the pressure will be imposed by the overall gas pocket behaviour. The semi-analytical model proposed in the next section should thus include this ability to condense at the wall. It is reasonable to consider that the larger the heat transfer, the larger the condensation and thus the larger the oscillation attenuation should be.

## SEMI-ANALYTICAL SOLUTION OF THE 1D COMPRESSION PROBLEM OF A GAS POCKET

### Theoretical model

Considering the remarks above, a simple semi-analytical model was developed, which allows for thermal transfers at the wall ( $z=0$ ) considering an exterior temperature  $T_{ext}$  and allows for the gas in the bottom cell to condense (or re-evaporate).

The liquid cell of Figure 4 is replaced by a solid piston of same mass and condensation or evaporation is neglected in the top cell. Figure 6 shows the new simplified model of the problem of Figure 4.

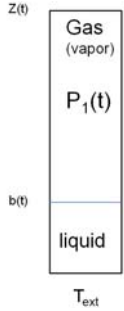


**Fig. 6** – Schematic description of the semi-analytical model

Due to heat transfers and compression, the gas (vapor) in the bottom cell may condensate at the wall.  $b(t)$  is the height of the small layer of liquid that will appear (Figure 6) while the location of the piston bottom is denoted by  $z(t)$ . The model also allows for liquid evaporation when the piston goes up, thus, provoking a depression.

The governing equations are obtained from basic principles.

The motion of the piston is given by:

$$\ddot{z}(t) = -g + \frac{1}{\rho_L h} (P_1(t) - P_2(t)) \quad (19)$$

where  $P_1$  and  $P_2$  are respectively the pressures in the bottom and top cells. In the same way  $\rho_1, \rho_2$  will denote the gas densities ( $\rho_G$ );  $T_1, T_2$  the temperatures in respectively the bottom and top cells.

A simple approximation of the heat exchanges is adopted with the differential equation:

$$\frac{dT}{dt} = -\kappa(T - T_{ext}) \quad (20)$$

where  $1/\kappa$  is a relaxation time. Furthermore Antoine's law (16) defines the saturation curve, with (17) involving explicitly the Jakob number.

As already announced, the evolution of the system is decomposed into two stages: a mechanical stage and a thermo-dynamical stage. The compression or expansion of the gas cells is assumed to be adiabatic and the mass of the gas is conserved during the mechanical stage. This stage enables a small move of the piston  $z+\delta z$  without any change of the liquid mass ( $b$  unchanged). A possible temporary imbalance of the gas pressures and densities will be solved by a transfer of mass between the two phases, if required by the relative position of the gas pressure with regards to the saturation curve.

The non-linear differential equations are solved numerically by a time domain discretization. Quantities at time step  $n$  are labelled with  $n$ .

Assuming that  $n$  time steps of the whole process have already been calculated, let us describe the step  $(n+1)$ :

**During the mechanical phase**, mass conservation (no phase change in this stage) gives:

$$\rho_1(z - b_n) = \rho_1^n(z_n - b_n), \quad \rho_2(H - h - z) = \rho_2^n(H - h - z_n).$$

Assuming an adiabatic evolution for the gas in this stage, one has

$$P_1(t) = P_1^n \left( \frac{z_n - b_n}{z(t) - b_n} \right)^\gamma, \quad P_2(t) = P_2^n \left( \frac{H - h - z_n}{H - h - z(t)} \right)^\gamma$$

and  $P_k \rho_k T_0 = P_0 \rho_k T_k$  with label 0 referring to initial ambient conditions where  $z_0 = z(0) = h_1, \dot{z}(0) = 0, b_0 = 0$ .

We set:  $z_{n+1} = z(t_{n+1}), \dot{z}_{n+1} = \dot{z}(t_{n+1}),$

$$\pi^{n+1} = P_1^n \left( \frac{z_n - b_n}{z_{n+1} - b_n} \right)^\gamma, \quad r_1^{n+1} = \rho_1^n \left( \frac{z_n - b_n}{z_{n+1} - b_n} \right), \quad \Theta_1^{n+1} = T_1^n \left( \frac{z_n - b_n}{z_{n+1} - b_n} \right)^{\gamma-1}$$

and analogous formulas for  $P_2^{n+1}, \rho_2^{n+1}$  and  $T_2^{n+1}$ .

$\Pi_k^{n+1}, r_k^{n+1}$  and  $\Theta_k^{n+1}$  are the evaluation of  $p_k, \rho_k$  and  $T_k$  after the mechanical stage.

**During the thermo-dynamical stage**,  $b$  is allowed to vary from  $b_n$  to  $b_{n+1}$  (phase transition). The mass conservation becomes:

$$\rho_1^{n+1}(z_{n+1} - b_{n+1}) + \rho_L(b_{n+1} - b_n) = r_1^{n+1}(z_{n+1} - b_n). \quad (21)$$

As the gas is on the saturation curve, Antoine's law (16) and relation (17) apply:

$$P_1^{n+1} = P_0 \exp\left(\frac{\gamma}{(\gamma-1)Ja} \left(1 - \frac{T_0}{T_1^{n+1}}\right)\right)$$

Since, according to (20), we have  $T_1^{n+1} = T_{ext} + \frac{\Theta_1^{n+1} - T_{ext}}{1 + \kappa(t_{n+1} - t_n)}$ ,

$P_1^{n+1}$  and thus  $\rho_1^{n+1}$  are obtained thanks to the EoS  $P_1^{n+1} r_1^{n+1} \Theta_1^{n+1} = \Pi^{n+1} \rho_1^{n+1} T_1^{n+1}$ . Finally  $b_{n+1}$  is found via (21).

### The oscillation killer suspect

The results obtained in the case of methane and its vapor at scale 1 are presented, both when considered along the phase boundary at atmospheric pressure and when considered as non-condensable fluids. Figure 7 shows the history of the piston motion and of the thickness of the liquid layer at the wall for  $\kappa = 10$ .

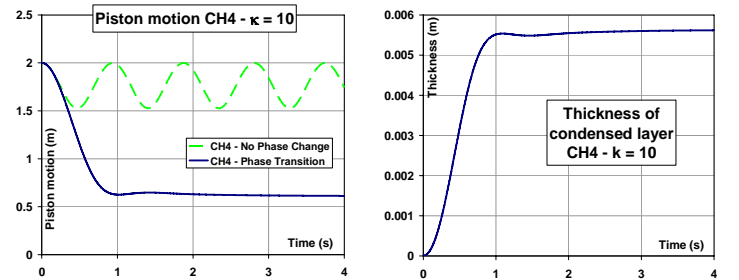


**Fig. 7** – Left: piston motion for methane with phase transition (blue) and without phase transition (green) – Right: thickness of the condensate gas at the wall (when phase transition is present) -  $\kappa = 10$ .

For a non-condensable gas (Figure 7 – left – green curve), the free fall of the piston together with the compression of the bottom cell (and the expansion of the top cell) creates a mass/spring system inducing regular oscillations of the piston. For the methane on the phase boundary, a thin layer of condensate will progressively accumulate along the wall while the piston keeps falling regularly until it reaches an equilibrium

position due to the expansion of the top cell. At the end a 6 mm thick layer of liquid at the wall has been generated. All oscillations have been killed. With an infinite length of the top cell, or fixing  $P_2=P_0$ , the piston would follow its fall down to the bottom and the whole gas would be transformed into liquid.

Figure 8 presents the comparison of the pressure time histories obtained in both cases.

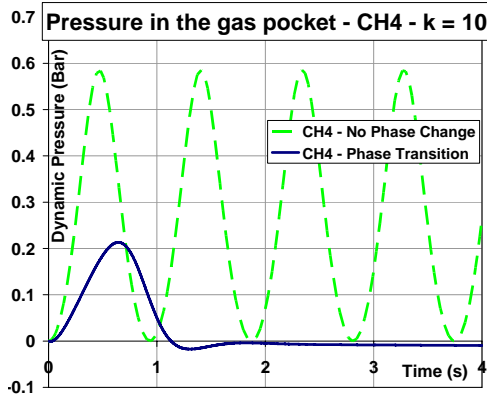


**Fig. 8** – Pressure time histories at the bottom for methane with phase transition (blue) and without phase transition (green) -  $\kappa = 10$  – (same parameters as in Fig.7).

The pressure history within the gas pocket is approximately a sine curve when no phase change is considered. For more violent impact conditions (higher density of the liquid or lower ullage pressure), the model would lead to sharp pressure peaks but necessarily followed by oscillations as the gas cannot escape. When the phase change is active, the oscillations disappear and the maximum pressure is strongly reduced.

Everything occurs as though the gas pocket were punctured and the compression had forced the gas to escape from it (here to become liquid). This case is an ideal one and considering different values of  $Ja$  and different thermal boundary conditions (values of  $\kappa$ ) leads to different results as illustrated in Figure 9 when  $\kappa=2$  is used with methane.

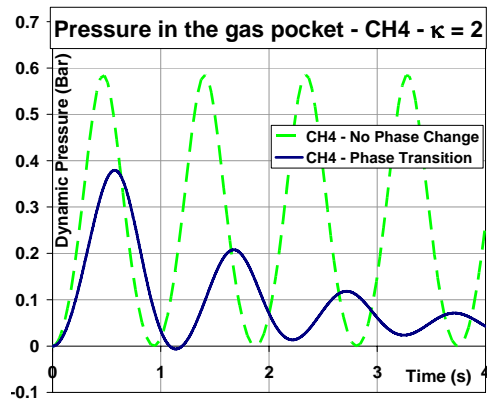


**Fig. 9** – Pressure time histories at the bottom for methane with phase transition (blue) and without phase transition (green) -  $\kappa = 2$

Nevertheless, it is reasonable to think that the gradual condensation at the wall during the compression of the gas pockets due to a thermal boundary layer explains both the strong reduction of the oscillations and the reduction of maximum pressures observed during the steam SMT. Furthermore the intuitive explanation given by Maillard *et al.* (2009) matches very well the process described here.

A candidate for *killing oscillations* has been clearly identified. The

condensation at the wall damps strongly the oscillations. At the same time the maximum pressures are reduced.

## General results on dimensionless form of the equations

In order to compare with sloshing impacts, only the configuration of the model for which  $h_2$  is infinite and the pressure in the top gas cell remains  $p_0$ , is interesting.

Dimensionless parameters  $z^*$ ,  $b^*$ ,  $t^*$ ,  $p^*$ ,  $T^*$ ,  $\rho_G^*$ ,  $\rho_L^*$  are defined respectively for  $z$ ,  $b$ ,  $t$ ,  $p$ ,  $T$ ,  $\rho_G$ ,  $\rho_L$ , based on the reference dimensional values  $h_1$  for the length,  $\sqrt{h_1/g}$  for the time,  $p_0$ ,  $T_0$ ,  $\rho_{G0}$  for respectively the pressure, the temperature and the density. In particular, we chose to have:

$$p^* = (p-p_0)/p_0 \text{ and } T^* = (T-T_0)/T_0$$

The equations governing the problem become in dimensionless form :

**During the mechanical phase:**  $b^*$  constant and  
 $\ddot{z}^*(t) = -1 + p^*(t)/S$  for the piston motion,

$\rho_G^*(z^*-b^*)=1$  and  $p^*=(z^*-b^*)^{-\gamma}-1$ ,  $p^* = -1 + \rho_G^*(1+T^*)$ , for the gas behaviour.

**During the thermo-dynamical phase:**  $z^*$  constant and

$\rho_G^*(z^*-b^*) + \rho_L^* b^* = 1$  for the mass transfer between phases,  
 $\partial T^*/\partial t^* = -\kappa^*(T^* - T_{ext}^*)$ , with  $\kappa^* = \kappa \sqrt{h_1/g}$  for the heat transfer,

$p^* = -1 + \exp\left(\frac{\gamma}{(\gamma-1)Ja}\left(\frac{T^*}{T^*+1}\right)\right)$  for the saturation law.

The problem is thus entirely governed by five dimensionless numbers:

$$S, Ja, \kappa^*, T_{ext}^*, DR = 1/\rho_L^*$$

- $DR = \rho_G/\rho_L$  is the density ratio between gas and liquid,
- $T_{ext}^*$  is the dimensionless external temperature and reflects the gap between the external temperature and the saturation temperature at nominal ullage pressure
- $\kappa^*$  governs the heat transfer for a given  $T_{ext}^*$
- $Ja$  is the Jacob number
- $S = \rho_L g h/p_0$  reflects the violence of the impacts from the global flow parameters. It is called *Impact Number* as Ramkema, (1978), proposed first for a similar 1D model.

The results for non-condensable gases depend only on  $S$ . A complete analysis is proposed by Bogaert, Brosset, Léonard and Kaminski (2010) in that case for a similar 1D model of gas pocket compression. Their model is without gravity but with an initial velocity of the piston that initiates the compression of the gas pocket. The results are presented in dimensionless form based on another impact number  $S$  suitable for their model.

In the case of a fluid on the phase boundary, a complete study could be made with the simple 1D model with independent variations of the six dimensionless numbers using virtual fluids. This would be useful if the model could prove first that the phase transition has a significant influence at full scale with LNG/NG.

For the time being the numerical solution has been developed with simplified assumptions in order to quickly check whether condensation is a good candidate or not for the destruction of oscillations and for the maximum pressure reduction observed during the steam SMT. For example, a constant time step, identical for the two stages (mechanics and thermodynamics) of the simulation has been used. Doing so roughly, the solution is not numerically stable and does not allow yet for large variations of the five dimensionless numbers. For example large values of  $S$  (violent impacts), that are the most important from the designer point of view, have not been tested yet. For water/steam the

range of  $S$  for which a stable solution was reached is even smaller. Therefore, simple improvements of the numerical solution have to be brought in order to enable all relevant variations of the dimensionless parameters that govern the problem.

The first priority will be to compare the behavior at full scale with LNG/NG to the behavior at small scale with water/steam (conditions of the steam tests).

When the fluids are fixed, DR,  $T_0$  and  $Ja$  are fixed. Considering a same reference outer temperature  $T_{ext} = 293.15\text{ K}$  ( $20^\circ\text{C}$ ) for both fluids,  $T_{ext}^*$  is thus also fixed. Only the violence of the impact (through  $S$ ) and the quality of the insulation (through  $\kappa^*$ ) is to be studied.

The model should allow to determine  $p_{max}(S, \kappa^*)$ ,  $f(S, \kappa^*)$ ,  $\delta(S, \kappa^*)$ , where  $p_{max}$ ,  $f$  and  $\delta$  are respectively the maximum pressure in the gas pocket, the frequency of its oscillations and its damping coefficient. Results will be presented at the conference.

## CONCLUSIONS

A clear pressure signature had been observed during Sloshing Model Tests with water and steam in a pressure vessel at varying saturation conditions for gas pocket impacts (Maillard *et al.*, 2009): as with non-condensable gases, the pressure for all sensors within a gas pocket gave exactly the same signal but the typical oscillations of the pressure signal had totally disappeared for all such numerous impacts. Furthermore the statistical pressures obtained from a relevant sample of pressure peaks turned out to be significantly smaller with water and steam than with water and a non-condensable gas, all other things being equal. The reason was clearly associated with the phase transition during the compression of the gas pockets. However, as both the pressure and the temperature increase according to the equation of state of the gas during the pocket compression, it was not easy to determine whether condensation of the gas phase due to the increase of the pocket pressure or evaporation of the liquid at the interface due to the increase of temperature was the main cause, as the boundary between the fluids moved on the saturation curve. Condensation was intuitively preferred because any attempt to overcome the saturation pressure would be to immediately *saturate*.

Rather than launching immediately long and costly tests, GTT wanted to check whether the attenuation of the pressure oscillations and the reduction of pressure could be demonstrated in principle by means of a simple semi-analytical 1D model of a gas pocket compression that could be considered as an extension of the well known Bagnold model.

Such a model has been developed by ENS-Cachan favouring the condensation at the wall by a parametric thermal transfer, as also observed by Goldstein in 1964 during shock tube tests with water-vapour. In the case of LNG + NG along the phase boundary, the 1D analytical model of gas pocket compression clearly showed the trends observed during the steam tests. Instead of oscillating regularly as with a non-condensable gas, the compression of the NG pocket induced the gradual growth of a thin layer of condensate at the wall while the piston fell without any oscillations. At the end of the piston fall, the gas entirely transformed into liquid. The pressure time history is greatly modified compared to the signal with non-condensable gas: the maximum pressure is significantly reduced, the time duration of the peak is increased and the oscillations are absent. As suggested by Maillard *et al.*, everything happens as though the gas pocket was punctured, the vapor leakage being replaced by the transformation to liquid.

This case was rather ideal. More often the oscillations are greatly damped but not killed, depending on the different values of the parameters involved. The mathematical formulation can be completely written in a dimensionless form by use of five dimensionless numbers

in addition to the Froude number, instead of one unique additional number for the same model without phase transition. This main number is the impact number  $S$  governing the violence of the impact (see Rameka, 1978, and Bogaert, Brosset, Léonard, Kaminski, 2010). Another number, which is already needed for a good similarity between sloshing model tests and full scale reality onboard LNG ships, is the density ratio (DR) between the vapor phase and the liquid phase. Here, DR rules the transfer of mass during the phase transition. The Jakob number ( $Ja$ ) governs the saturation law and finally two other numbers govern the heat transfer at the wall.

The numerical solution developed recently for the theoretical model is quite rough but allowed to find quickly the main suspect for the massive gas pocket oscillation destruction. The solution is not numerically stable and does not allow yet for a study of the five dimensionless numbers with a sufficiently large range.

When the fluids within the 1D tank are fixed and the external temperature is also fixed, only the violence of the impact (through the  $S$  number) and the quality of the insulation (through a heat transfer number  $\kappa^*$ ) is to be studied.

After improving the numerical solution, the model should enable to determine  $p_{max}(S, \kappa^*)$ ,  $f(S, \kappa^*)$ ,  $\delta(S, \kappa^*)$ , where  $p_{max}$ ,  $f$  and  $\delta$  are respectively the maximum pressure in the gas pocket, the frequency of its oscillations and its damping coefficient.

In parallel to the 1D model study, CFD developments are in progress in order to simulate liquid impacts in 2D with fluids along the phase boundary. The Flux-IC software (Braeunig, Desjardin, Ghidaglia, 2009) is a two compressible phase solver with an advanced free surface tracking method. Improvements have been undertaken in order to include the physics of phase transition into the model. At the same time different thermal boundary conditions are to be developed in addition to the already existing isentropic condition.

As the designer of the membrane containment systems for LNG tanks, the main objective of GTT remains the safety of its solutions onboard LNG ships. It has to be checked carefully whether the phase transition could be, in certain conditions to be determined, an amplifying phenomenon of the sloshing impact pressures. Up to now, through the steam sloshing model tests and through the first results of the 1D model of vapour compression, the phase transition looks as a mitigating effect that is not taken into account during the sloshing model tests, therefore adding implicitly a safety factor to the tests results.

## REFERENCES

- Bagnold, R., (1939). *Interim report on wave-pressure research*, J. Inst Civil Eng. **12**: 201–226.
- Bogaert, H., Brosset, L., Léonard, S., Kaminski, M., (2010), "Sloshing and scaling: results from Sloshel project", 20<sup>th</sup> (2010) Int. Offshore and Polar Eng. Conf., Beijing, China, ISOPE.
- Bogaert, H., Léonard, S., Marhem, M., Leclère, G., Kaminski, M., (2010), "Hydro-structural behavior of LNG containment systems under breaking wave impacts: findings from the Sloshel project", 20<sup>th</sup> (2010) Int. Offshore and Polar Eng. Conf., Beijing, China, ISOPE.
- Braeunig, J.-P., Brosset, L., Dias, F., Ghidaglia, (2009) "Phenomenological study of liquid impacts through 2D compressible two-fluid numerical simulations", 19<sup>th</sup> (2009) Int. Offshore and Polar Eng. Conf., Osaka, Japan, ISOPE.
- Braeunig, J.-P., Desjardins B., Ghidaglia, J.-M., (2009). "A totally Eulerian finite volume solver for multi-material fluid flows", European Journal of Mechanics-B/Fluids **28**, 475-485.
- Braeunig, J.-P., Brosset, L., Dias, F., Ghidaglia, J.-M., Maillard, S., (2010) "On the scaling problem for impact pressure caused by



*sloshing*”, in preparation for a scientific journal, (May 2010?).

Brosset, L., Mravak, Z., Kaminski, M., Collins, S., Finnigan, T., (2009) “*Overview of Sloskel project*”, 19<sup>th</sup> (2009) Int. Offshore and Polar Eng. Conf., Osaka, Japan, ISOPE.

Dias, F., Brosset, L., (2010). “*Comparative Numerical Study: description of the calculation cases*”, 20<sup>th</sup> (2010) Int. Offshore and Polar Eng. Conf., Beijing, China, ISOPE.

Dias, F., Ghidaglia, J.-M., Le Coq, G., (2007). “*On the fluid dynamics for sloshing*”, ISOPE, 2007-1129 (2007)

Faghri, A., Zhang, Y., (2006). “*Transport Phenomena in Multiphase Systems*”, Elsevier, 2006.

Faltinsen, O.M., Timokha, A.N. (2009). “*Sloshing*”, Cambridge University Press.

Goldstein, R. (1964), “*Study of water vapor condensation on shock-tube walls*”, The Journal of Chemical Physics 40, 2793-2799.

Ishii, M., Hibiki, T., (2006). “*Thermo-Fluid Dynamics of Two-Phase Flow*”, Springer, New-York, 2006.

Landau, L.D., Lifshitz, E.M. (1987), “*Fluid mechanics*”, Second Edition: Volume 6, Pergamon Press, Oxford, UK.

Maillard, S., Gervaise, E., de Sèze, P.-E., Brosset, L. (2010). “*New methodology used by Gastransport & Technigaz for liquid motion studies*”, External document n°??

Maillard, S., Brosset, L., (2009). “*Influence of Density Ratios between liquid and gas on sloshing model test results*”, 19<sup>th</sup> (2009) Int. Offshore and Polar Eng. Conf., Osaka, Japan, ISOPE.

Oger, Brosset, L., Guilcher, P.-M., Jacquin, E., G., Deuff, J.-B., Le Touzé, D., (2009). “*Simulations of hydro-elastic impacts using a parallel SPH model*”, 19<sup>th</sup> (2009) Int. Offshore and Polar Eng. Conf., Osaka, Japan, ISOPE.

Oger, Brosset, L., Guilcher, P.-M., Jacquin, J.-B., Le Touzé, D., (2010). “*Simulation of Liquid Impacts with a Compressible Two-phase Parallel SPH Model*”, 20<sup>th</sup> (2010) Int. Offshore and Polar Eng. Conf., Beijing, China, ISOPE.

Ramkema, C., (1978). “*A model law for wave impacts on coastal structures*”, Proceedings of 16<sup>th</sup> International Conference on Coastal Engineering, August 27-31, Hamburg, Germany.

Copyright ©2010 The International Society of Offshore and Polar Engineers (ISOPE). All rights reserved.